Original paper

Julgoldite-(Fe^{2+}) and Fe-rich prehnite from pectolite veins at Košťálov quarry, Czech Republic: Mössbauer, WDS and PXRD study

Luboš VRTIŠKA[1]*, Jiří SEJKORA[1], Jaromír TVRDÝ[1], Jan FILIP[2], Jan LOUN[3], Radana VRTIŠKOVÁ[1]

[1] *Department of Mineralogy and Petrology, National Museum, Cirkusová 1740, 193 00, Praha 9, Czech Republic; lubos.vrtiska@nm.cz*
[2] *Regional Centre of Advanced Technologies and Materials, Czech Advanced Technology and Research Institute (CATRIN), Palacký University, Šlechtitelů 27, 779 00 Olomouc, Czech Republic*
[3] *KYOCERA AVX Components s.r.o., Dvořákova 328, 563 01 Lanškroun, Czech Republic*
** Corresponding author*

Julgoldite-(Fe^{2+}) and Fe-rich prehnite were found in pectolite veins filling fissures in basaltic andesite at the Košt'álov quarry near Semily (Liberec region, Czech Republic). Empirical formula of julgoldite-(Fe^{2+}) based on EPMA and Mössbauer spectroscopy considering so-called intervalence electron hopping in the structure may be written as $Ca_{2.01}(Fe^{2+}_{0.56}Fe^{2.5+}_{0.25}Mg_{0.14})_{\Sigma 0.95}(Fe^{3+}_{1.19}Fe^{2.5+}_{0.25}Al_{0.57})_{\Sigma 2.01}Si_3O_{9.94}(OH)_{4.06}$. Refined unit-cell parameters for monoclinic space group A2/m are a = 8.927(3) Å, b = 6.080(2) Å, c = 19.428(7) Å, β = 97.59(4)°, V = 1045.2(8) Å^3. Prehnite with the empirical formula $Ca_{2.01}(Al_{0.53}Fe_{0.45})_{\Sigma 0.98}(AlSi_3O_{10})(OH)_{1.93}F_{0.02}$ is located approximately in the middle of the prehnite-ferriprehnite series. Mössbauer spectroscopy indicated that all Fe is present in the trivalent form. The increased Fe content is also reflected in this unit-cell: a = 18.617(5) Å, b = 5.502(2) Å, c = 4.672(2) Å, V = 478.5(2) Å^3. Pectolite is the main mineral in the mineral assemblage. Its unit-cell parameters refined from powder X-ray diffraction are a = 7.9848(14) Å, b = 7.0391(19) Å, c = 7.0243(11) Å, α = 90.53(2)°, β = 95.19(1)°, γ = 102.48(2)° and V 383.7(1) Å^3. Chemical composition of pectolite corresponds to ideal stoichiometry and give the empirical formula $Na_{1.00}(Ca_{2.02}Mn_{0.01}Fe_{0.01})_{\Sigma 2.04}Si_3O_8(OH_{1.04})F_{0.02}$. Other minor minerals of the association are hematite, pyrite and the youngest calcite. The source of mineralization of the circulating fluids can be found in alteration of rock components (feldspars, olivine, glass); however, external input from the surrounding calcareous sediments cannot be excluded.

Keywords: pumpellyite group minerals, julgoldite-(Fe^{2+}), Fe-rich prehnite, basaltic andesite, Mössbauer study, Košťálov, Czech Republic
Received: 5 May 2025; accepted: 3 September 2025; handling editor: M. Števko

1. Introduction

Julgoldite-(Fe^{2+}) is a very rare mineral from the pumpellyite group with ideal formula $Ca_2Fe^{2+}Fe^{3+}_2[Si_2O_6OH][SiO_4](OH)_2(OH)$. The general formula of pumpellyite groups minerals is $W_2XY_2Z_3O_{14-n}(OH)_n$ with $4 \geq n \geq 3$ (Passaglia and Gottardi 1973; Nagashima et al. 2018). The *W* sites are predominantly occupied by Ca; in the *Z* sites dominant Si may be partially substituted by Al (Passaglia and Gottardi 1973). The *Y* site is occupied by trivalent cations Al, Fe^{3+}, Mn^{3+}, V^{3+}, Cr^{3+} and prevailing cation in this site determined root name of the species (Tab. 1). In general, both divalent and trivalent cations, such as Mg, Al, Mn^{2+}, Mn^{3+}, Fe^{2+}, Fe^{3+}, V^{3+}, and Cr^{3+}, occupy the *X* site; the dominant element at *X* site is appended as suffix to the root name (Passaglia and Gottardi 1973; Nagashima et al. 2018).

Julgoldite-(Fe^{2+}) and Fe-rich prehnite in association with calcite, hematite and pyrite in veins of white, cream, light pink or rare light blue pectolite were found in the active quarry in Košťálov, Czech Republic. Pectolite forms continuous fracture fillings in the rock composed of radially arranged needle-like silky, shiny crystals up to 3 cm long. In narrow central cavities, small, well-developed clear crystals of pectolite rise from the pectolite aggregates. Younger julgoldite-(Fe^{2+}) and Fe-rich prehnite grow on pectolite and together with calcite, hematite and pyrite fill the spaces between pectolite needles. Sometimes the cavities in pectolite are covered with up to a 3 mm thick crust of finely crystalline beige calcite or

Tab. 1 Ideal occupation of crystal structure sites of pumpellyite group minerals

Y (2 *apfu*)	*X* (1 *apfu*)	Name
Al	Al	pumpellyite-(Al)
Al	Fe^{2+}	pumpellyite-(Fe^{2+})
Al	Fe^{3+}	pumpellyite-(Fe^{3+})
Al	Mg	pumpellyite-(Mg)
Al	Mn^{2+}	pumpellyite-(Mn^{2+})
Fe^{3+}	Fe^{2+}	julgoldite-(Fe^{2+})
Fe^{3+}	Fe^{3+}	julgoldite-(Fe^{3+})
Fe^{3+}	Mg	julgoldite-(Mg)
Mn^{3+}	Mn	okhotskite
V^{3+}	V	poppiite
Cr^{3+}	Mg	shuiskite-(Mg)
Cr^{3+}	Cr	shuiskite-(Cr)

Y, *X* – sites of the general formula $W_2XY_2Z_3O_{14-n}(OH)_n$, *W* – Ca dominant

there this mineral forms up to 2 mm large rhombohedral crystals. Second generation of pectolite forming colourless needle-like crystals up to 5 mm long in some of cavities is the youngest observed mineral of the assemblage.

2. Geological setting

The quarries in the Želechovské valley west of the village of Košt'álov (Liberec Region, Czech Republic; GPS position: 50°33'50.627"N, 15°22'50.941"E) are known for the occurrence of various mineral associations on fractures of Permo–Carboniferous basaltic andesite ("melaphyre"). Especially the pectolite samples are one of the best in the Czech Republic (Gotthard 1933; Kašpar 1941; Tuček 1965; Kašpar et al. 2010). Other minerals have been described from the locality together with pectolite or in separate associations. There were found prehnite, baryte, fluorapophyllite-(K), hydroxylapophyllite-(K), stevensite, calcite, andradite, datolite and chalcedony; of the zeolites, chabazite-Ca, heulandite-Ca, scolecite, stellerite and thomsonite-Ca are listed (Kratochvíl 1930; Kašpar 1942; Tuček 1943; 1965; Faust et al. 1959; Pauliš et al. 2020; Tvrdý et al. 2023; Vrtiška et al. 2024). An occurrence of copper mineralization (djurleite, chrysocolla, brochantite) in Košťálov is discussed by Pauliš and Malec (2010).The Košt'álov quarry is located about 6 km southeast of the centre of the town of Semily. The area is a part of the Krkonoše basin, one of the fault-bounded late Paleozoic intramontane (Piedmont basin type) troughs in the northeastern part of the Bohemian Massif, Czech Republic. The basin fill comprises the Upper Carboniferous (Westphalian)

Fig. 1 Part of vein consisting of fibrous creamy pectolite (lower part), with grains of light green Fe-rich prehnite, radial aggregates of dark green to black julgoldite-(Fe^{2+}) and beige calcite from the Košťálov quarry. Sample dimensions 70 × 65 mm.

to Lower Permian continental volcano-sedimentary succession, overlain by uppermost Permian (Zechstein) and Mesozoic marine deposits (Dostal et al. 2020). The basin hosts two main cycles of volcanism. To the older, Late Carboniferous (~307 Ma) cycle belong relatively modest amounts of volcanic rocks of mainly intermediate compositions (trachyandesite). The second, Lower Permian major cycle produced effusions and shallow intrusions of more basic tholeiitic rocks traditionally called melaphyres (basalts, basaltic andesites, andesites), locally overlain by ignimbrites and rarely rhyolite lavas dated at ~297 Ma (Ulrych et al. 2003, 2006; Opluštil et al. 2016; Dostal et al. 2020). A part of the younger complex is an intrusive body that stretches for about 10 km from the slope of the Kozákov Hill through Hořensko, Stružinec to Libštát. The body is discordantly emplaced in red aleuropelites and sandstones of the Lower Permian (Knotek and Bašta 1976). At Košťálov, the rock of basaltic andesite composition is subject to intensive quarrying for the production of crushed aggregate since 1922.

Fig. 2 Dark red radial aggregates of hematite up to 1 mm in size growing into fibrous aggregates of dark green julgoldite-(Fe^{2+}) from the Košťálov quarry. Field of view 11 mm.

3. Methods

Powder X-ray diffraction data (PXRD) were measured by Bruker D8 Advance diffractometer (National Museum, Prague) with a solid-state 1D LynxEye

Fig. 3 Fibrous aggregates of dark green julgoldite-(Fe^{2+}) overgrown with pyrite, colourless pectolite and yellow calcite. Field of view 5 mm.

detector (width 2.05°) using Cu*K*α radiation and operating at 40 kV and 40 mA. The powder patterns were collected using Bragg–Brentano geometry in the range 5–70° 2θ, in 0.01° steps with a counting time of 8 s per step. X-ray powder diffraction data were processed using the program HighScore Plus, where the profile fitting was done using a Pseudo-Voigt profile shape function corrected for asymmetry (full-axial model). Obtained positions of the diffraction maxima were used for the refinement of the unit-cell parameters by the Celref program of the

Tab. 2 Chemical composition of julgoldite-(Fe^{2+}) (wt. %, *apfu*)

			Mean	1	2	3	4	5	6	7
	CaO		20.84	20.59	21.02	20.70	21.28	20.86	20.90	20.56
	FeO	1*	10.79	10.69	10.84	11.12	10.21	10.55	11.13	10.99
	MgO		1.05	1.03	1.01	1.04	1.01	1.00	1.19	1.08
	MnO		0.03	0.00	0.06	0.00	0.00	0.05	0.06	0.05
	Al_2O_3		5.37	5.82	5.57	4.75	6.98	5.98	3.97	4.52
	Fe_2O_3	1*	21.32	21.12	21.42	21.98	20.17	20.85	21.98	21.72
	SiO_2		33.42	33.60	33.59	33.28	33.69	33.48	33.10	33.19
	H_2O	2*	6.78	6.88	6.72	6.75	6.56	6.74	6.87	6.94
	Total		99.60	99.74	100.22	99.61	99.90	99.51	99.19	99.06
	Fe^{2+}	3*	0.563	0.554	0.562	0.582	0.528	0.549	0.586	0.577
	$Fe^{2.5+}$	3*	0.495	0.488	0.495	0.513	0.465	0.483	0.515	0.508
	Fe^{3+}	3*	1.193	1.175	1.192	1.235	1.119	1.164	1.242	1.223
W site	Ca		2.005	1.969	2.012	2.000	2.030	2.002	2.030	1.991
X site	Fe^{2+}		0.563	0.554	0.562	0.582	0.528	0.549	0.586	0.577
	$Fe^{2.5+}$		0.248	0.244	0.248	0.256	0.232	0.242	0.258	0.254
	Mg		0.141	0.137	0.135	0.139	0.134	0.133	0.161	0.146
	Mn^{2+}		0.002	0.000	0.005	0.000	0.000	0.004	0.004	0.004
	Σ		0.953	0.936	0.949	0.978	0.894	0.928	1.009	0.980
Y site	Fe^{3+}		1.193	1.175	1.192	1.235	1.119	1.164	1.242	1.223
	$Fe^{2.5+}$		0.248	0.244	0.248	0.256	0.232	0.242	0.258	0.254
	Al		0.568	0.612	0.586	0.504	0.733	0.632	0.424	0.482
	Σ		2.008	2.031	2.026	1.995	2.084	2.037	1.923	1.959
	Si		3.000	3.000	3.000	3.000	3.000	3.000	3.000	3.000
	O		9.941	9.903	9.999	9.942	10.102	9.973	9.846	9.819
	OH		4.059	4.097	4.001	4.058	3.898	4.027	4.154	4.181

Mean of 7 point analyses; 1–7 individual point analyses; *apfu* on the basis of Si = 3. Notes: 1* FeO and Fe_2O_3 contents were recalculated on the base of results of Mössbauer spectroscopy ($Fe^{2.5+}$ was converted to Fe^{2+} and Fe^{3+}); 2* content of H_2O calculated on the base of general formula and charge balance; 3* Fe contents on the base of results of Mössbauer spectroscopy (Fe^{2+} 24% D4+D5; $Fe^{2.5+}$ 22% D3; Fe^{3+} 53% D1 + D2).

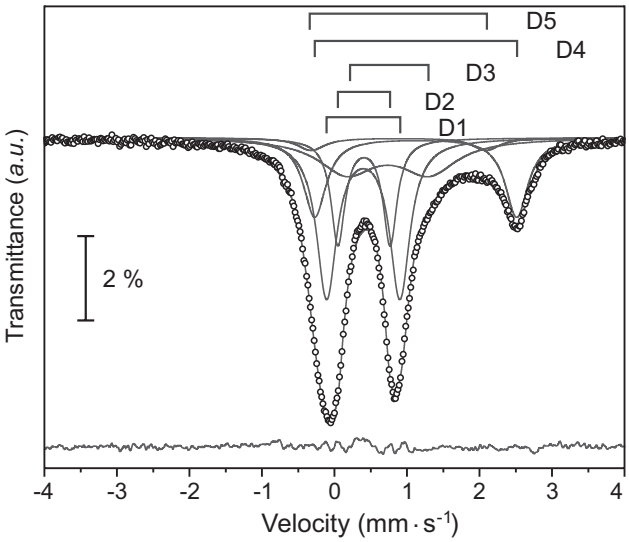

Fig. 4 ^{57}Fe Mössbauer spectrum of julgoldite-(Fe^{2+}) from Košťálov. For hyperfine parameters and assignment of particular doublets see Tab. 3.

LMGP suite for Windows (Laugier and Bochu 2011), an algorithm based on least-squares method.

The chemical composition of studied minerals was determined on polished and carbon-coated fragments mounted in an epoxy cylinder using a Cameca SX 100 electron microprobe (EPMA) at Faculty of Science, Masaryk University Brno. The instrument was operated in wavelength-dispersive mode at accelerating voltage of 15 kV, beam current of 10 nA, and beam diameter of 8 μm for julgoldite-(Fe^{2+}) and hematite, and 10 μm for prehnite and pectolite. The following X-ray lines and standards were selected; *K*α lines: Na (albite), Si, Al, K (sanidine), Mg (pyrope), Cl (vanadinite), Ti (titanite), Cr (chromite), Ca (wollastonite), Fe (almandine), Mn (spessartine), V ($ScVO_4$), Zn (gahnite), F, (topaz), Ni (syn. Ni_2SiO_4); *L*α lines: Ba (baryte), Sr (syn. $SrSO_4$). Contents of K, Mg, Cl, Ti, Cr, V, Ni Ba and Sr were below detection limits (~0.05–0.10 wt. %). Counting times were 10–20 s on peak and half of this time for each background position. The raw intensities were converted to the concentrations automatically using *PAP* (Pouchou and Pichoir 1985) matrix-correction software. Water could not be analysed directly because of the very small amount of material available; the H_2O content was calculated by stoichiometry of ideal formulas.

Mössbauer spectra on isotope ^{57}Fe of powdered julgoldite and prehnite samples were collected at room-temperature using a conventional spectrometer (constant acceleration mode, transmission geometry) equipped with a ^{57}Co (in Rh matrix) radioactive source (1.85 GBq) at Palacký University Olomouc. Carefully hand-picked mineral fragments were ground under isopropyl alcohol to avoid iron oxidation. The values of hyperfine parameters (i.e., isomer shift values) were calibrated against a rolled metallic iron (α-Fe) foil at room temperature. The spectrum was fitted by Lorentz functions using the CONFIT2000 software (Žák and Jirásková 2006). The experimental error is ± 0.02 mm s^{-1} for the hyperfine parameters and ± 3 % for the relative spectral areas.

4. Results

4.1. Julgoldite-(Fe^{2+})

Julgoldite-(Fe^{2+}) was not yet described from the territory of the Czech Republic. In Košťálov, this mineral forms radial crystal aggregates up to 7 mm in size in association with hematite, Fe-rich prehnite, small cubes and grains of pyrite up to 1 mm in size and calcite in spaces between pectolite aggregates (Fig. 1–3). The mineral is black, greenish black to dark green with vitreous lustre, perfect cleavage and olive-green colour in thin section.

The results of chemical analyses of julgoldite-(Fe^{2+}) from Košťálov (Tab. 2) agree with general stoichiometry of pumpellyite groups minerals with Ca contents ranging from 1.97 to 2.03 *apfu*, *X* + *Y* cations 2.93–2.98 *apfu* and calculated *n* value (OH groups) in the range 3.90–4.18 *pfu*. The Fe^{2+} and Fe^{3+} contents were derived from results of Mössbauer spectroscopy (see below). The *Y* site is dominantly occupied by Fe^{3+} (with minor Al in the range 0.42–0.73 *apfu*) and therefore the root name is julgoldite (Tab. 1). The occupation of *X* site is rather complicated, besides prevailing Fe^{2+} (0.53–0.59 *apfu*) also contents of formal Fe$^{2.5+}$ (0.23–0.26 *apfu*), Mg (0.13–0.16 *apfu*) and traces of Mn were observed. The empirical formula of julgodite-(Fe^{2+}) from Košťálov may be written as $Ca_{2.01}(Fe^{2+}_{0.56}Fe^{2.5+}_{0.25}Mg_{0.14})_{\Sigma 0.95}(Fe^{3+}_{1.19}Fe^{2.5+}_{0.25}Al_{0.57})_{\Sigma 2.01}Si_3O_{9.94}(OH)_{4.06}$.

The ^{57}Fe Mössbauer spectrum of julgoldite from Košťálov was fitted with 5 paramagnetic doublet components (Fig. 4), corresponding clearly to Fe^{2+} (25 % of total iron) and Fe^{3+} (53 % of total iron), as well as to iron with delocalized electrons (so-called intervalence electron hopping – Fe$^{2.5+}$, 22%; for typical hyperfine parameters of Fe$^{2.5+}$ in silicate structures see e.g. Andreozzi et al. 2008). Based on

Table 3 Parameters of the ^{57}Fe Mössbauer spectrum of julgoldite-(Fe^{2+}) from Košťálov

Doublet	Isomer shift, mm s^{-1}	Quadrupole splitting, mm s^{-1}	Line width, mm s^{-1}	Relative area, %	Assignment
D1	0.40	1.01	0.33	36	Fe^{3+} (*Y*-site)
D2	0.41	0.72	0.23	17	Fe^{3+} (*Y*-site)
D3	0.74	1.13	0.93	22	Fe$^{2.5+}$ (X/*Y*-site)
D4	1.12	2.79	0.38	21	Fe^{2+} (X-site)
D5	0.89	2.41	0.46	4	Fe^{2+} (X-site)

Tab. 4 Powder X-ray diffraction data of julgoldite-(Fe^{2+})

h	*k*	*l*	d_{obs}	I_{obs}	d_{calc}
0	0	2	9.631	1	9.629
1	0	0	8.886	74	8.849
–1	0	2	7.000	7	6.991
1	0	2	6.136	7	6.125
–1	1	1	4.917	2	4.940
0	0	4	4.808	25	4.815
1	1	1	4.756	3	4.763
2	0	0	4.440	85	4.424
–2	0	2	4.250	13	4.238
–1	1	3	4.091	1	4.101
1	0	4	4.012	2	4.013
2	0	2	3.843	100	3.833
–2	1	1	3.580	1	3.587
–2	0	4	3.498	19	3.496
2	1	1	3.451	1	3.452
0	1	5	3.261	1	3.254
0	2	0	3.036	85	3.040
1	1	5	2.960	64	2.949
–2	0	6	2.777	40	2.778
–3	0	4	2.676	1	2.677
3	1	1	2.5885	2	2.5877
–3	1	3	2.5587	21	2.5622
2	0	6	2.4518	2	2.4489
–1	0	8	2.4030	1	2.4047
–3	1	5	2.3174	1	2.3177
–2	0	8	2.2399	11	2.2425
–4	0	2	2.2209	75	2.2209
–4	0	4	2.1237	24	2.1191
1	2	6	2.0970	6	2.0972
–3	1	7	2.0336	2	2.0345
–4	0	6	1.9479	10	1.9454
4	0	4	1.9133	8	1.9165
3	2	4	1.8758	4	1.8735
–3	1	9	1.7727	3	1.7717
4	1	5	1.7412	3	1.7413
–3	0	10	1.7209	4	1.7198
–2	3	5	1.6988	1	1.6988
–3	3	3	1.6485	1	1.6467
4	2	4	1.6210	8	1.6212
–1	0	12	1.6171	7	1.6170
0	0	12	1.6043	6	1.6049
–5	1	7	1.5331	4	1.5353
3	2	8	1.5179	2	1.5199
3	3	5	1.4926	<1	1.4922
0	3	9	1.4717	2	1.4714
6	1	1	1.4156	<1	1.4159
–1	0	14	1.3878	2	1.3873
–3	1	13	1.3639	1	1.3643

combination of hyperfine parameters of particular doublets (Tab. 3) with chemical data from EMPA and taking into account hyperfine parameters published for various julgoldite-pumpellyite samples (e.g. Akasaka et al. 1997; Nagashima et al. 2006; Nagashima et al. 2018) we assign all Fe^{3+} (and 1/2 of $Fe^{2.5+}$) to occupy *Y* site (i.e., 64 % of iron atoms) and all Fe^{2+} (and 1/2 of $Fe^{2.5+}$) to occupy *X* site (i.e., 36 % of iron atoms). There is no spectral evidence for Fe^{3+} in magnetically ordered compounds as impurities (e.g., hematite).

The experimental powder XRD data for julgodite-(Fe^{2+}) from Košťálov quarry (Tab. 4) agree well with the data published by Allmann and Donay (1973). The refined unit-cell parameters correspond to published data for this mineral phase (Tab. 5) and follow the trend of increasing values depending on Fe contents (or mean ionic radius) in *Y* site observed by Akasaka et al. (1997) and Nagashima et al. (2018).

4.2. Fe-rich prehnite

The occurrence of Fe-rich prehnite containing 7–8 wt. % FeO_{tot} in Košťálov is already mentioned by Pauliš et al. (2020). In the studied samples, it occurs in semi-transparent light green spherical aggregates up to 15 mm in size with vitreous to low pearly lustre, brittle tenacity and weak cleavage (Fig. 1). The chemical composition (Tab. 6) corresponds to ideal prehnite stoichiometry, beside low contents of Zn (up to 0.01 *apfu*) and F (up to 0.02 *apfu*), significant Fe contents in the range 0.41–0.49 *apfu* (mean 0.45) were determined. Increased contents of Fe (up to 0.43–0.46 *apfu*) are known especially in prehnites from Mitsu, Japan (Nagashima et al. 2017), Kouragahana (Akasaka et al. 2003), Komiža (Balić-Žunić et al. 1990) and Mali (Detrie et al. 2008). Mean value 0.66 apfu Fe (0.43–0.79) is reported for the mineral ferriprehnite (Nagashima et al. 2021). Empirical formula of studied prehnite from Košťálov (mean of 6 point analyses) on the base of 3 Si *apfu* is $Ca_{2.01}(Al_{0.53}Fe_{0.45})_{\Sigma 0.98}(AlSi_3O_{10})(OH)_{1.93}F_{0.02}$.

Table 7 shows a comparison of refined unit-cell parameters for prehnite from Košťálov with published data for minerals of prehnite–ferriprehnite series. The positive correlation between Fe content and cell volume (Fig. 5) is consistent with the observations of Nagashima et al.

Tab. 5 Unit-cell parameters of julgoldite-(Fe^{2+}) refined for monoclinic space group *A*2/*m*

Locality	Reference	*a* [Å]	*b* [Å]	*c* [Å]	*β*[°]	*V* [Å^3]
Košťálov (CZ)	this paper	8.927(3)	6.080(2)	19.428(7)	97.59(4)	1045.2(8)
Långban (SWE)	Allmann and Donnay (1973)	8.922(4)	6.081(3)	19.432(9)	97.60(6)	1045.02
Tafjord (NOR)	Brastad (1984)	8.949	6.047	19.426	97.38	1041.92
Kaulbach/Kreimbach (GER)	Nagashima et al. (2018)	8.9454(3)	6.0519(2)	19.4008(5)	97.589(2)	1041.10(3)
Bombay (IND)	Nagashima et al. (2018)	8.9034(4)	6.0568(3)	19.3580(9)	97.584(3)	1034.77(4)

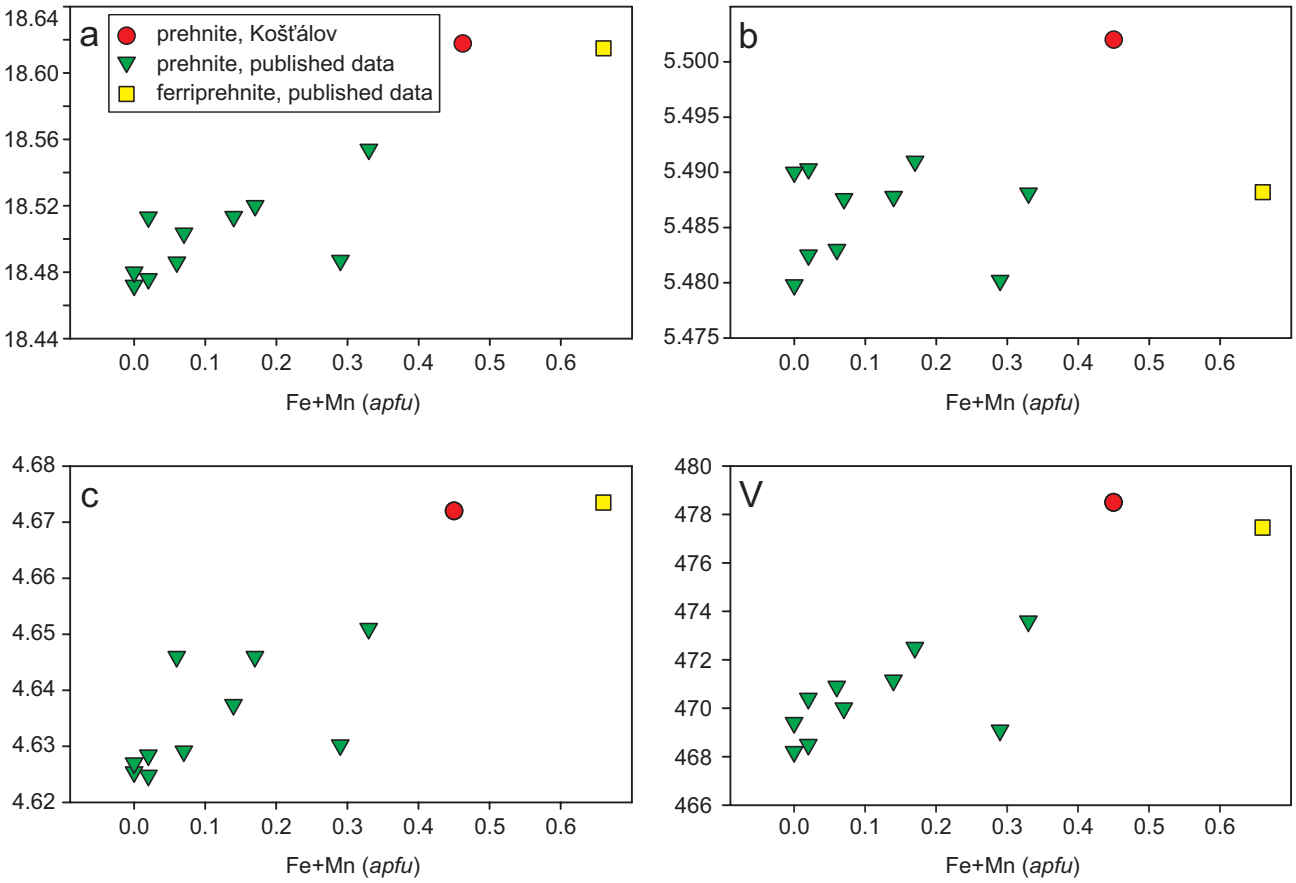

Fig. 5 Variations of the unit-cell parameters [Å] *vs*. total Fe (+Mn) content (*apfu*) of prehnite and ferriprehnite; published data are taken from Tab. 7.

(2017); moreover, the same relation of the *b* parameter is also evident.

The ^{57}Fe Mössbauer spectrum of prehnite from Košťálov (Fig. 6) was fitted with one narrow doublet with hyperfine parameters (isomer shift δ = 0.37, quadrupole splitting ΔE_Q = 0.29 mm/s, line width Γ = 0.36 mm/s) corresponding exclusively to Fe^{3+} at octahedral structural site. This observation is comparable to the previous spectroscopic studies on Fe-rich prehnite samples from Mitsu

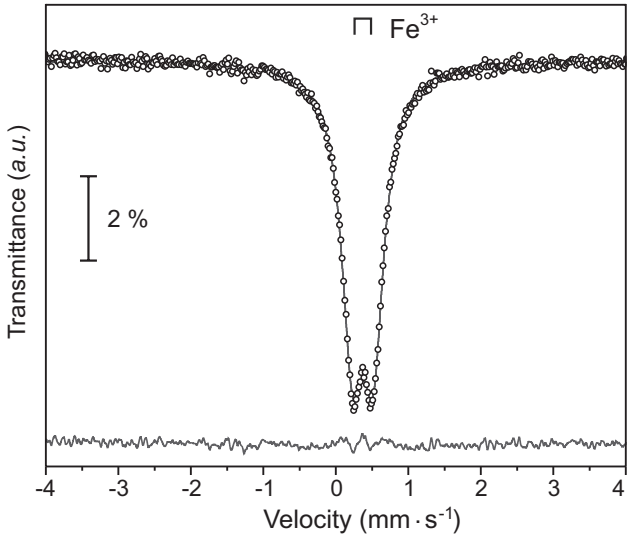

Fig. 6 ^{57}Fe Mössbauer spectrum of ferrian prehnite from Košťálov.

Tab. 6 Chemical composition of prehnite from Košťálov (wt. %, *apfu*)

	Mean	1	2	3	4	5	6
CaO	26.21	26.54	26.49	26.08	25.79	26.64	25.74
ZnO	0.05	0.13	0.08	0.07	0.05	0.00	0.00
Fe_2O_3	8.27	7.63	7.95	8.20	8.27	8.46	9.08
Al_2O_3	18.13	18.42	18.43	18.28	17.85	18.43	17.36
SiO_2	41.90	41.51	41.37	42.17	42.52	42.00	41.84
F	0.09	0.09	0.07	0.11	0.10	0.08	0.08
O=F	–0.04	–0.04	–0.03	–0.05	–0.04	–0.03	–0.03
H_2O*	4.05	4.26	4.42	3.95	3.51	4.36	3.78
Total	98.66	98.53	98.77	98.81	98.04	99.94	97.84
Ca	2.011	2.055	2.058	1.988	1.950	2.038	1.978
Zn	0.003	0.007	0.004	0.003	0.002	0.000	0.000
Σ	2.014	2.062	2.062	1.991	1.952	2.038	1.978
Fe	0.445	0.415	0.434	0.439	0.439	0.455	0.490
Al	0.530	0.569	0.575	0.532	0.485	0.551	0.467
Σ	1.975	1.983	2.009	1.972	1.924	2.006	1.957
Al	1.000	1.000	1.000	1.000	1.000	1.000	1.000
Si	3.000	3.000	3.000	3.000	3.000	3.000	3.000
F	0.020	0.020	0.016	0.025	0.022	0.019	0.018
OH	1.934	2.054	2.138	1.874	1.652	2.077	1.808

Coefficients of empirical formula calculated on the base 3 Si *apfu*; H_2O* content calculated on charge balance.

Tab. 7 The unit-cell parameters for members of prehnite–ferriprehnite series

Mineral*	Locality	Reference	Fe+Mn	SG**	*a* [Å]	*b* [Å]	*c* [Å]	*V* [Å^3]
Prh	Košťálov	this paper	0.45	*Pma*2	18.617(5)	5.502(2)	4.672(2)	478.5(2)
Fprh	Kouragahana	Nagashima et al. (2021)	0.66	*Pma*2	18.6149(10)	5.4882(3)	4.6735(3)	477.46(1)
Prh	Mitsu	Nagashima et al. (2017)	0.33	*Pma*2	18.5540(4)	5.4881(1)	4.6510(1)	473.59
Prh	Kouragahana	Akasaka et al. (2003)	0.29	*Pmna*	18.487(1)	5.4802(3)	4.6302(3)	469.09(5)
Prh	Komiža	Balić-Žunić et al. (1990)	0.17	*P2cm*	18.52(3)	5.491(3)	4.646(2)	472.5
Prh	Mitsu	Nagashima et al. (2017)	0.14	*Pma*2	18.5134(4)	5.4878(1)	4.6374(1)	471.15(2)
Prh	Tyrol	Detrie et al. (2008)	0.07	*Pncm*	18.5034(15)	5.4876(6)	4.6291(5)	470.0(7)
Prh	Tyrol	Papike and Zoltai (1967)	0.06	*Pncm*	18.486(5)	5.483(2)	4.646(2)	470.9
Prh	South Africa	Detrie et al. (2008)	0.02	*Pncm*	18.5131(13)	5.4903(4)	4.6284(3)	470.4(7)
Prh	Kuruman	Detrie et al. (2009)	0.02	*Pncm*	18.476(1)	5.4825(4)	4.6248(4)	468.5
Prh	Norway	Detrie et al. (2008)	0.00	*Pncm*	18.472(4)	5.4798(10)	4.6254(8)	468.2(7)
Prh	Radautal	Preisinger (1965)	0.00	*P2cm*	18.48	5.490	4.627	469.4

* Prh – prehnite, Fprh – ferriprehnite; ** SG – published space group, for comparison were all parameters transformed to setting *Pma*2

and Kouragahana, Japan (Nagashima et al. 2017; Akasaka et al. 2003).

4.3. Pectolite and hematite

Among the minerals accompanying julgodite-(Fe^{2+}) and Fe-rich prehnite, attention was paid to pectolite and hematite.

Pectolite as the main component of the vein filling (Fig. 1) was confirmed by PXRD and EPMA. Its unit-cell parameters refined for triclinic space group *P*-1 from the powder X-ray diffraction pattern, *a* 7.9848(14) Å, *b* 7.0391(19) Å, *c* 7.0243(11) Å, *α* 90.53(2)°, *β* 95.19(1)°, *γ* 102.48(2)° and *V* 383.7(1) Å^3, agree well with the published data (Prewitt 1967). Chemical composition of pectolite (Tab. 8) corresponds to ideal stoichiometry; only minor contents of Fe, Mn (up to 0.02 *apfu*) and F (up to 0.03 *apfu*) were found. Its empirical formula (mean of 8 point analyses) on the basis of 3 Si *apfu* is $Na_{1.00}(Ca_{2.02}Mn_{0.01}Fe_{0.01})_{\Sigma 2.04}Si_3O_8(OH_{1.04})F_{0.02}$.

Rare hematite forms dark red radial inclusions up to 1 mm in size in julgoldite-(Fe^{2+}) aggregates or in pectolite cavities where it grows with calcite (Fig. 2). Hematite was determined by PXRD and EPMA. Its unit-cell parameters for trigonal space group *R*-3*c* refined from powder X-ray diffraction, *a* 5.0381(14), *c* 13.7544(4) Å and *V* 302.34(8) Å^3, are consistent with those for typical hematite (Blake et al. 1966). Its chemical composition (mean of 3 point analyses), CaO 0.13, Fe_2O_3 98.50, Al_2O_3 0.29, SiO_2 1.39, total 100.32 wt. %, corresponds to hematite with only minor contents of Si (0.04 *apfu*) and Al (0.01 *apfu*).

5. Discussion and conclusions

The identification of Fe-rich members of the pumpellyite and prehnite groups at Košt'álov near Semily (Czech Republic) points to an enhanced role of iron in the younger members of the rock-fracture mineral association with a dominant pectolite. Attention is paid in particular to the role of Fe in the structure of both julgoldite and Fe-rich prehnite, based on the results of valence state determination by Mössbauer spectroscopy. In the julgoldite-(Fe^{2+}) spectrum, 25 % of the total Fe was assigned to Fe^{2+}, 53% to Fe^{3+} and the remaining 22 % to iron with delocalized electrons. Interestingly, pectolite, the most abundant

Tab. 8 Chemical composition of pectolite (wt. %)

	Mean	1	2	3	4	5	6	7	8
Na_2O	9.22	8.93	9.37	9.35	9.11	9.45	8.95	9.47	9.15
CaO	33.60	33.87	33.56	33.49	33.76	33.67	33.40	33.44	33.64
FeO	0.12	0.00	0.13	0.19	0.05	0.00	0.00	0.32	0.23
MnO	0.24	0.10	0.16	0.20	0.40	0.13	0.51	0.19	0.24
SiO_2	53.60	53.78	54.18	53.15	53.22	53.69	53.51	53.78	53.48
F	0.12	0.14	0.13	0.11	0.13	0.16	0.10	0.11	0.10
H_2O*	2.79	2.69	2.69	2.89	2.91	2.78	2.71	2.82	2.85
O=F	-0.05	-0.06	-0.06	-0.05	-0.06	-0.07	-0.04	-0.05	-0.04
Total	99.64	99.44	100.17	99.32	99.52	99.80	99.14	100.09	99.65
Na	1.001	0.966	1.006	1.023	0.996	1.023	0.973	1.024	0.995
Ca	2.015	2.024	1.991	2.025	2.039	2.016	2.006	1.998	2.022
Fe	0.005	0.000	0.006	0.009	0.002	0.000	0.000	0.015	0.011
Mn	0.011	0.004	0.008	0.009	0.019	0.006	0.024	0.009	0.011
Σ	2.032	2.029	2.005	2.043	2.061	2.022	2.030	2.022	2.044
Si	3.000	3.000	3.000	3.000	3.000	3.000	3.000	3.000	3.000
F	0.022	0.025	0.023	0.020	0.024	0.029	0.018	0.020	0.017
OH	1.042	1.001	0.994	1.088	1.094	1.036	1.013	1.049	1.066

Coefficients of empirical formula calculated on the base 3 Si *apfu*; H_2O* content calculated on charge balance.

mineral of the studied association, contains only minor Fe contents (up to 0.015 *apfu*). The structure of pectolite, like other pyroxenoids of the wollastonite group, probably incorporates Fe only to a very limited extent. Currently, only ferrobustamite as a member of the wollastonite group contains Fe in the ideal formula. However, it is found in different geological conditions, especially in contact metamorphosed skarns, and is stable at high temperatures (Rapoport and Burnham 1973).

The described mineral association developed during post-magmatic low-temperature phases in a fissure-permeable rock body. The solutions circulating along the fractures in the basaltic andesite were enriched by chemical substances resulting from the decomposition of rock components (feldspars, olivine, glass); the addition of substances from the surrounding calcareous sediments cannot be ruled out.

Acknowledgements. The authors wish to express their thanks to Radek Škoda (Masaryk University, Brno) for kind support in this study. Jan Bubal (Museum of Bohemian Paradise, Turnov) and Petr Pauliš (Kutná Hora) are thanked for valuable information about the locality. This work was financially supported by the Ministry of Culture of the Czech Republic (long-term project DKRVO 2024-2028/1.II.b; National Museum, 00023272).

References

Akasaka M, Kimura Y, Omori Y, Sakabira M, Shinno I, Togari K (1997) ^{57}Fe Mössbauer study of pumpellyite–okhotskite–julgoldite series minerals. Mineral Petrol 61: 181–198

Akasaka M, Hashimoto H, Makino K, Hino R (2003) ^{57}Fe Mössbauer and X-ray studies of ferrian prehnite from Kouragahana, Shimane Peninsula, Japan. J Mineral Petrol Sci 98: 31–40

Allman R, Donnay G (1973) The crystal structure of julgoldite. Mineral Mag 39: 271–281

Andreozzi GB, Bosi F, Longo M (2008) Linking Mössbauer and structural parameters in elbaite–schorl–dravite tourmalines. Am Mineral 93: 658–666

Balić-Žunić T, Šćavničar S, Molin G (1990) Crystal structure of prehnite from Komiža. Eur J Mineral 2: 731–734

Blake RK, Hessevick RE, Zaltai T, Finger LW (1966) Refinement of the hematite structure. Am Mineral 51: 124–129

Brastad K (1984) Julgoldite from Tafjord, Sunnmøre. Contribution to the Mineralogy of Norway, No. 67. Nor Geol Tidsskr 64: 251–255

Detrie TA, Ross NL, Angel RJ, Welch MD (2008) Crystal chemistry and location of hydrogen atoms in prehnite. Mineral Mag 72: 1163–1179

Detrie TA, Ross NL, Angel RJ, Gatta GD (2009) Equation of state and structure of prehnite to 9.8 GPa. Eur J Mineral 21: 561–570

Dostal J, Shellnutt JG, Ulrych J (2020) Petrogenesis of post-collisional Late Paleozoic volcanic rocks af the Bohemian Massif (Central Europe): Isotopic variations of the lithospheric mantle related to Variscan orogeny. Lithos 354–355: 105331

Faust GT, Hathaway JC, Millot GA (1959) A restudy of stevensite and allied minerals. Am Mineral 44(3–4): 342–370

Gotthard J (1933) Petrografická povaha melafýrů podkrkonošských. Arch Přírodověd Výzk Čech (Praha) 18(2): 1–65 (in Czech)

Kašpar JV (1941) Pektolith ze Želechovského údolí u Libštátu. Pektolith aus dem Želechov – Tal bei Liebstadtl. Zpr Geol Úst Čechy Mor 17: 42–49 (in Czech)

Kašpar JV (1942) Hanušit, nový nerost. Chem Listy 36: 78–81 (in Czech)

Kašpar P, Řídkošíl T, Rajlich P, Ulrych J (2010) Pektolit z Želechovského údolí u Libštátu. Sbor Muz Čes Ráje Turnov 4: 92–98 (in Czech)

Knotek Z, Bašta J (1976) Závěrečná zpráva úkolu Košťálov-východ 511 1383 506. Surovina: kámen (melafýr). Geoindustria, Praha. MS ČGS, Geofond FZ005555 (in Czech)

Kratochvíl J (1930) Minerální bohatství širokého Turnova. Od Ještěda k Troskám 9(1–2): 5–21 (in Czech)

Laugier J, Bochu B (2011) LMGP-Suite of Programs for the interpretation of X-ray experiments. Accessed on April, 2011, at http://www. ccp14.ac.uk/tutorial/lmgp

Nagashima M, Ishida T, Akasaka M (2006) Distribution of Fe among octahedral sites and its effect on the crystal structure of pumpellyite. Phys Chem Miner 33: 178–191

Nagashima M, Iwasa K, Akasaka M (2017) Crystal chemistry and oxidation state of Fe-rich prehnite from a hydrothermally altered dolerite. Mineral Petrol 112(2): 173–184

Nagashima M, Cametti G, Armbruster T (2018) Crystal chemistry of julgoldite, a mineral series of the pumpellyite group: re-investigation of the Fe distribution and hydrogen-bonding. Eur J Mineral 30: 721–731

Nagashima M, Nishio-Hamane D, Ito S, Tanaka T (2021) Ferriprehnite, $Ca_2Fe^{3+}(AlSi_3)O_{10}(OH)_2$, an Fe^{3+} analogue of prehnite, from Kouragahana, Shimane Peninsula, Japan. J Mineral Petrol Sci 116: 129–139

Opluštil S, Schmitz M, Kachlík V, Štamberg S (2016) Re-assessment of lithostratigraphy, biostratigraphy and volcanic activity of the Late Paleozoic Intra-Sudetic, Krkonoše-Piedmont and Mnichovo Hradiště basins (Czech Republic) based on new U–Pb CA-ID-TIMS ages. Bull Geosci 91(2): 399–432

Papike JJ, Zoltai T (1967) Ordering of tetrahedral aluminum in prehnite. $Ca_2(Al,Fe^{3+})[Si_3AlO_{10}](OH)_2$. Am Mineral 52: 974–984

Pauliš P, Malec J (2010) Výskyt Cu-mineralizace v permském melafyru od Košťálova u Semil (Podkrkonošská pánev, Česká republika). Bull Mineral-Petrolog Odd Nár Muz (Praha) 18(2): 106–108 (in Czech)

Pauliš P, Malý J, Malý T, Pour O (2020) Nové nálezy minerálů v kamenolomu v Košťálově u Semil. Minerál 27(4): 296–299 (in Czech)

Passaglia E, Gottardi G (1973) Crystal chemistry and nomenclature of pumpellyites and julgoldites. Canad Mineral 12: 219–223

Pouchou J, Pichoir F (1985) "PAP" (ϕρZ) procedure for improved quantitative microanalysis. In: Armstrong JT (ed): Microbeam Analysis. San Francisco Press, San Francisco, pp 104–106

Preisinger A (1965) Prehnit – ein neuer Schichtsilikattyp. Tschermaks Mineral Petrogr Mitt 10(1–4): 491–504

Prewitt CT (1967) Refinement of the structure of the pectolite, $Ca_2NaHSi_3O_9$. Z Kristallogr 125: 298–316

Rapoport PA, Burnham CW (1973) Ferrobustamite: The crystal structures of two Ca,Fe bustamite-type pyroxenoids. Z Kristallogr 138: 419–438

Tuček K (1943) Nové nálezy nerostů I. Věst Král Čes Spol Nauk, Tř Math-Přírodověd 6: 1–32 (in Czech)

Tuček K (1965) O nálezech pektolitu v Čechách a na Moravě. Čas Nár Muz, Odd Přírodověd 134: 105–110 (in Czech)

Tvrdý J, Vrtiška L, Dolníček Z, Malíková R (2023) Stellerit z Košťálova u Semil (Česká republika). Bull Mineral Petrolog 32(2): 209–216 (in Czech)

Ulrych J, Štěpánková J, Novák JK, Pivec E, Prouza V (2003) Volcanic activity in Late Variscan basins of northern Bohemia: petrological and geochemical constraints. Slovak Geol Mag 33: 219–235

Ulrych J, Pešek J, Štěpánková-Svobodová J, Bosák P, Loyd FE, Von Seckendorf V, Lang M, Novák JK (2006) Permo–Carboniferous volcanism in late Variscan continental basins of the Bohemian Massif (Czech Republic): geochemical characteristic. Chem Erde 66(1): 37–56

Vrtiška L, Tvrdý J, Dolníček Z, Dvořák Z (2024) Andradit a datolit z Košťálova u Semil (Liberecký kraj, Česká republika). Bull Mineral Petrolog 32(1): 85–94 (in Czech)

Žák T, Jirásková Y (2006) CONFIT: Mössbauer spectra fitting program. Surf Interface Anal 38: 710–714